Polymer Bulletin (2026) 83:279
https://doi.org/10.1007/s00289-026-06338-0

ORIGINAL PAPER

Characterization study on mechanical, thermal conductivity and water absorption properties of silane-modified *Plumbago zeylanica* stem fiber and wheat straw extracted biosilica particle reinforced polyester composite

P. Subash[1] · P. Gurusamy[1] · V. Muthuraman[2] · S. Vijayan[3]

Received: 2 July 2025 / Revised: 10 January 2026 / Accepted: 16 February 2026

Abstract

Human development in past few decades are growing rapidly and their demands over earth sources are also increased rapidly. This resulted exploitation of natural resources and creation of pollution due to utilization of large fuel consuming heavy metals. To provide solution to this lightweight composite material are preferred in most of industrial and transport vehicle sectors. This present study aims to develop a lightweight polymer composite using surface modified *Plumbago Zeylanica* stem fiber and wheat straw biosilica reinforced polyester matrix. The utilization of natural source of reinforcement and that too after surface modification provide better strength and make unique sense to the composite material. To understand their performance the composites are developed based on hand layup process and testing such as mechanical, thermal conductivity and water absorption are done in accordance to the ASTM standard. The result of this composites shows that maximum tensile, flexural, ILSS, and IFSS strengths of 126 MPa, 162 MPa, 68 MPa and 18.9 MPa are obtained by the silane-modified stem fiber of 40 vol% and 3 vol% of silane-treated biosilica particle in the composite PNB2, which is 173.91%, 138.23%, and 277.77% better than plain composite P. The primary reason of these enhanced strength characteristics is the silane-treated fiber or filler's stronger connection with the matrix and it is better viewed through SEM analysis. Nevertheless, the composite PNB3 with 5 vol% modified biosilica reinforcement exhibits the highest impact and hardness strength of 5.85 J and 85 shore-d. Comparably, the same composite PNB3 with that volume percentage of surface-treated fiber and filler exhibits a reduced water absorption rate of 0.21% and a maximum thermal conductivity of 0.861 W/m-K, outperforming plain composite P by 209.71% and 61.90%, respectively. Thus, this light weight, better mechanical and thermal conductivity, water absorption properties of composites could potentially be applied in areas such as outer door panel works in automotive and aviation, enclosures setup

Extended author information available on the last page of the article

Published online: 28 February 2026

in power industrial sector, domestic household, and roof top work in civil engineering sector, etc.

Keywords Polymer composite · Fibre · Particle · Surface treatment · Mechanical properties · Thermal properties

Introduction

The modern world's demand for sustainability has driven the shift towards eco-friendly materials. However, conventional metals and alloys contribute to carbon emissions during production and degradation. Therefore, researchers are focusing on biodegradable alternatives such as biocomposites, which offer a promising solution due to their lightweight, cost-effectiveness, environmental friendliness, and good mechanical properties. Generally, biocomposite is made up of polymer matrix reinforced with natural fibers or particles from renewable biological sources. Among the components of biocomposites, natural fibers play a crucial role in reinforcing the polymer matrix andenhancing the strength properties of the composite. In addition, these fibers are obtained from various parts of plants, such as stems, roots, and leaves, effectively transforming biomass into valuable reinforcement materials. Specifically, fibers extracted from stems are preferred for their high cellulose content, better fiber length, and superior mechanical qualities [1]. In this research, *Plumbago zeylanica* stem fiber was utilized as the reinforcing material due to its high cellulose content (67–76%), which enhances the mechanical behaviour of the composite. Due to these advantages, several scholars have explored the wide range of natural fibers in their researches. Typically, Balogun et al. [2] investigated the *Entada mannii* stem fiber reinforced composite and resulted the tensile strength 63%, hardness of 49%, flexural strength 51%. In similar way, Okafor et al. [3] examined the *Dioscorea alata* stem fiber reinforced composite and showed the tensile strength of 94.2 MPa, and shear strength of 18.1 MPa in composite. Likewise, *Ficus benjamina L.* stem fiber reinforced composite was analysed by Joe et al. [4] and reported the impact strength of 9.31 kJ/m^2, tensile strength of 77.1 MPa, and flexural strength of 87.4 MPa respectively.

Even with their various benefits, natural fiber composites frequently experience void formation, which can compromise the structural integrity of composite. To overcome this issue, fillers are incorporated to enhance compactness, minimize defects, and improve the overall performance of the materials [5]. In this work, biosilica is used as a filler derived from wheat straw, a widely available agricultural by-product containing approximately 60–70% silica. This elevated silica content helps to boost the composite's strength, improve heat resistance, and enhances surface hardness. The application of biosilica and other biofillers to enhance the functional characteristics of polymer composites has been documented in several investigations. For instance, Ponnusamy et al. [6] evaluated the kenaf fiber and nanosilica filler reinforced composite and resulted the tensile strength of 31%, flexural strength of 42.36%, and impact strength of 22.65%. Similarly, silica particles and manila fiber reinforced composite was investigated by Venkatesh et al. [7] and showed the tensile

strength of 36.1 ± 0.36 MPa, and flexural strength of 76 ± 0.7 MPa was observed with the addition of 5 wt% silica particles. Correspondingly, *Amaranthus dubius* stem fiber and biosilica particles reinforced composite was assessed by Lakshmipathi et al. [8] and showed the shear strength of 154 MPa, sp. wear rate of 0.007 mm^3/Nm, and thermal conductivity of 0.812 W/mK was achieved with the inclusion of 2 vol% biosilica particles.

Although fiber and filler offer several advantages, they also present certain drawbacks such as weak interfacial bonding, which can reduce the strength of the composite. Hence, silane treatment is employed to enhance the interfacial interaction between the polymer matrix and the reinforcements. Moreover, silane coupling agents promote stronger adhesion and reduce water absorption [9]. Further, this research demonstrates that silane modification was applied to both the fiber and filler to improve their compatibility. Consequently, the use of silane-treated fiber and filler has been shown in several studies to enhance the strength and durability of composites. For example, Balaji et al. [10] investigated the silane treated basalt fiber reinforced composite and concluded the tensile strength of 133%. In the same way, Diharjo et al. [11] analysed the silane treatment on *Cordia dichotoma* fiber reinforced composites and showed the tensile strength of 105.37 MPa and modulus of elasticity 5.14 GPa was observed with the addition of 1 wt% of fiber. Likewise, alkali treated snake grass fiber reinforced polyester composite was examined by Jenish et al. [12] and resulted the tensile strength of 45 MPa, impact strength of 3.35 J, and hardness of 27 BHN.

The novelty claim of utilizing *Plumbago zeylanica* stem fiber and wheat-straw-derived biosilica is significant; however, its justification lies in the compositional and mechanical distinctiveness of this fiber compared with other commonly explored stem fibers. Plumbago zeylanica fiber, rich in cellulose and moderate lignin content, offers favourable stiffness, strength, and interfacial adhesion potential when properly surface-treated. Similarly, biosilica obtained from wheat straw provides a sustainable, thermally stable, and mechanically reinforcing filler derived from agricultural biomass waste. Based on the overall discussion, the integration of silane-treated natural fibers and biomass-derived fillers into polymer matrices is recognized as an effective and eco-friendly approach for advanced composite design. Accordingly, the objective of this research is to develop and characterize an epoxy-based biocomposite reinforced with silane-treated *Plumbago zeylanica* stem fiber and wheat-straw-derived biosilica particles. To the best of the authors' knowledge, no prior studies have reported the combined utilization of these specific reinforcements in polymer composites. Hence, this study addresses the existing research gap and establishes the novelty of the present work. The developed biocomposite demonstrates promising potential for applications in lightweight structural panels, packaging materials, and automotive interior components.

Materials and methodology

Materials

The present study use Unsaturated polyester resin and its corresponding catalyst methyl ethyl ketone peroxide (MEKP), used as the polymer matrix, obtained from Aarvi Marketing Pvt. Ltd., Chennai, India.The fiber reinforcement, *Plumbago Zeylanica* stems were purchased from Rishi Galav Herbs & Herbal Products, Madhya Pradesh, India. Wheat straw was sourced from Jyoti Herbals, Chennai, India, and processed into biochar, which were used as filler reinforcement in the composite. The silane treatment process utilized analytical-grade ethanol, acetic acid, and 3-APTMS were supplied by Ramdev general store, Chennai, India.

Fiber extracted from *Plumbago zeylanica* stem

The *Plumbago zeylanica* stems used for fiber reinforcement were purchased from Rishi Galav Herbs & Herbal Products, Madhya Pradesh, India. The extraction process began with cleaning the collected stems to remove dirt and contaminants, followed by cutting them into smaller pieces. To facilitate the breakdown of hemicellulose and lignin, the material was soaked in a sodium hydroxide (NaOH) solution and maintained at 85 °C for two and a half hours. The fibers were then thoroughly washed with distilled water until a neutral pH was reached [13]. Subsequently, they were dried in a hot air oven at 80 °C for five hours to eliminate residual moisture. Finally, the dried fibers were manually combed to remove entanglements and cut into uniform lengths of approximately 25–30 mm for use as reinforcement in composite fabrication. During layup, the fibers were randomly oriented to ensure uniform dispersion and to promote quasi-isotropic mechanical behavior. Figure 1 illustrates the *Plumbago zeylanica* stem fiber extraction process.

Biosilica filler extracted from wheat straw

Wheat straw was collected from a specified source, thoroughly washed with deionized water to remove dirt, and cut into small pieces. The cleaned straw was dried in a hot air oven at 110 °C for two hours. It was then subjected to slow pyrolysis in a muffle furnace at 950 °C for two hours. The resulting ash was mixed with 60 ml of 2 M sodium hydroxide (NaOH) solution in a 1:10 ratio. This mixture was heated in a water bath at 90 °C with continuous stirring to produce sodium silicate [14]. The solution was then cooled and filtered to obtain the sodium silicate extract. Subsequently, 2 M hydrochloric acid (HCl) was added to precipitate silica gel. Finally, the silica gel was aged for 24 h to improve gel structure and silica yield. After the aging process, the silica gel was bleached using a diluted hydrogen peroxide (H_2O_2) solution to eliminate residual colour and impurities. The purified biosilica particles were then obtained through filtering, washing, and drying. The filler extraction of biosilica from wheat straw was illustrated in Fig. 2 and the FESEM morphology of biosilica is presented in Fig. 3a). The particles are spherical and have sizes in the range between 20 and 30 nm. Similarly, Fig. 3b) presents the EDX mapping of the biosilica disper-

Fig. 1 *Plumbago Zeylanica* stem fiber extraction process

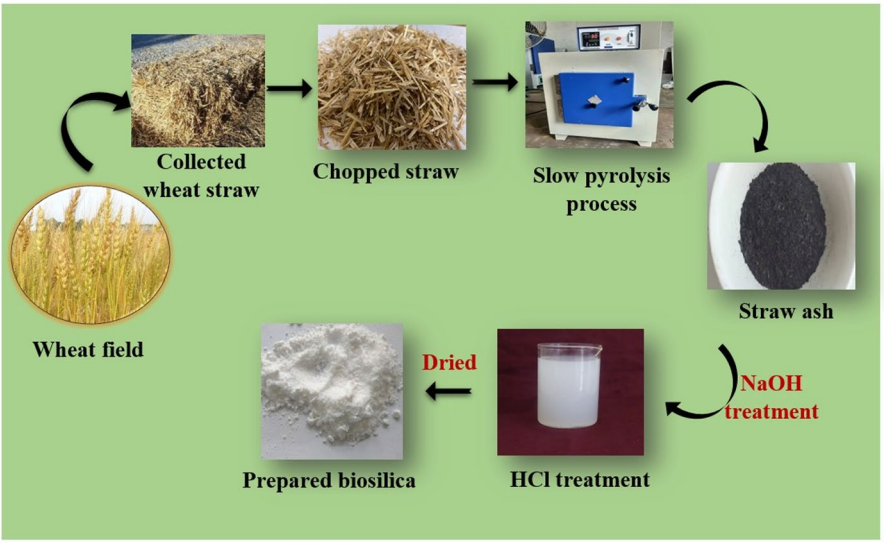

Fig. 2 Filler extraction of biosilica from wheat straw

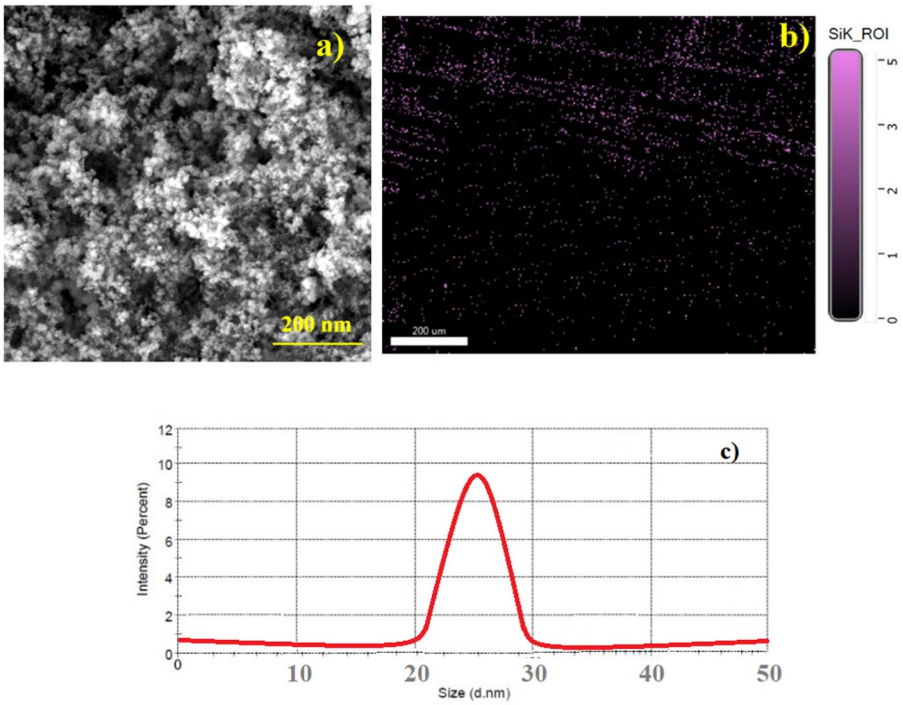

Fig. 3 (**a**) FESEM image, (**b**) EDX mapping and (**c**) PSA of biosilica from wheat straw

sion illustrating the uniform dispersion of the particles. Further, Fig. 3c) illustrates the particle size analyser offering insights on the particle size ranging from 20 to 30 nm.

Silane treatment on both fiber and filler reinforcement

Silane surface modification was applied to *Plumbago zeylanica* stem fiber and wheat straw–derived biosilica particles to enhance interfacial adhesion with the polyester matrix. A 2 wt% solution of 3-Aminopropyltrimethoxysilane (3-APTMS) was prepared in ethanol, and the pH was carefully adjusted to 4.0 ± 0.1 using a few drops of acetic acid, monitored with a digital pH meter. The fiber-to-solution ratio was maintained at 1:20 (g/mL), and continuous stirring was carried out at 400 rpm for 30 min to ensure uniform surface activation [15]. After treatment, the fibers and biosilica particles were filtered, thoroughly rinsed with distilled water to remove unreacted silane residues, and dried in a hot air oven at 60 °C for six hours. Following composite fabrication, post-curing was performed under mild vacuum conditions at 60 °C for four hours to minimize void formation and ensure effective matrix consolidation. The process flowchart of silane-modified *Plumbago zeylanica* stem fiber and wheat straw biosilica particles is presented in Fig. 4. The FTIR spectra of silane-modified *Plumbago zeylanica* stem fiber (Fig. 5a) showed characteristic peaks at ~3330 cm^{-1} (O–H stretching), 2915 cm^{-1} (C–H stretching), and 1100–1020 cm^{-1} corresponding

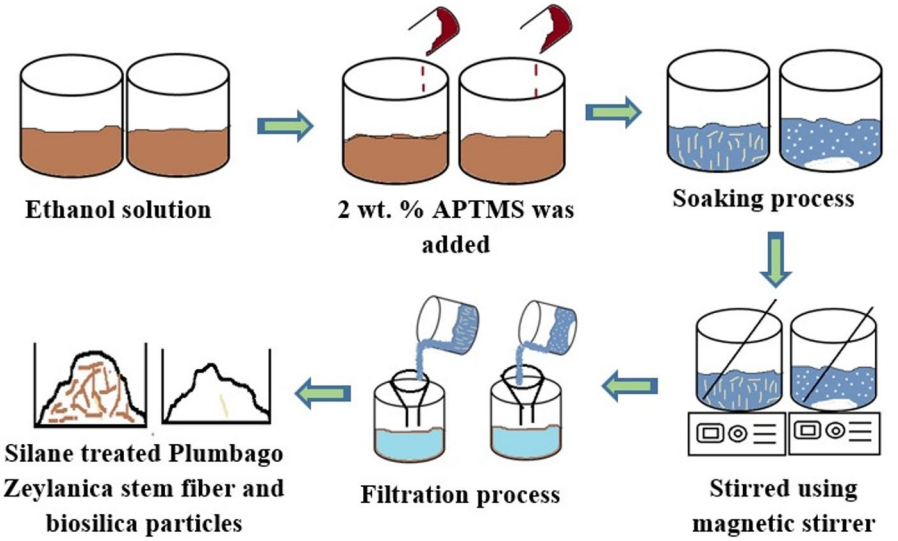

Fig. 4 Silane modified *Plumbago Zeylanica* stem fiber and wheat straw biosilica particles

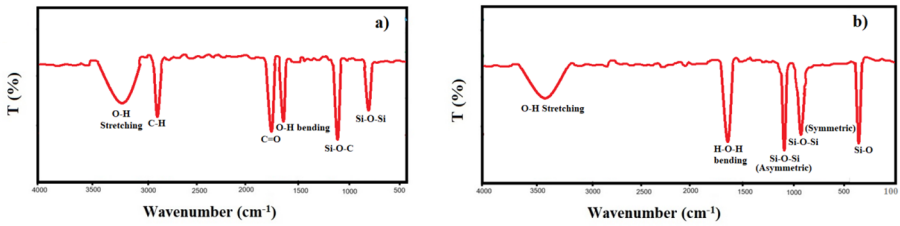

Fig. 5 FTIR spectra for (**a**) fiber and (**b**) filler particles

to Si–O–C linkages, confirming successful silane coupling with the fiber surface. The appearance of a Si–O–Si band around 780 cm^{-1} further indicated the formation of a siloxane network, while the reduced intensity of the O–H peak reflected decreased hydrophilicity. Similarly, the wheat straw–derived biosilica (Fig. 5b) exhibited prominent peaks at ~1080 cm^{-1} (asymmetric Si–O–Si stretching), 800 cm^{-1} (symmetric Si–O–Si stretching), and 460 cm^{-1} (Si–O bending), confirming the amorphous silica structure. The broad O–H band near 3440 cm^{-1} and the H–O–H bending at 1630 cm^{-1} were attributed to surface silanol groups and adsorbed moisture.

Preparation of composite

The hand lay-up method was employed for composite fabrication. The required quantity of polyester resin, determined based on the specific composite formulation, was first placed in a mixing container. The catalyst (methyl ethyl ketone peroxide) was then added in the specified weight ratio. Silane-treated *Plumbago zeylanica* stem fiber and biosilica particles derived from wheat straw were gradually incorporated

Table 1 Composite designation with varying concentration of reinforcements

Composite designation	Polyester resin (vol%)	Natural fiber (vol%)	Bio-silica (vol%)
P	100	-	-
PNB0	60	40	-
PNB1	59	40	1
PNB2	57	40	3
PNB3	55	40	5

Fig. 6 Process flowchart of composite development

into the resin matrix and uniformly dispersed using a mechanical stirrer [16]. To minimize air entrapment and void formation, the prepared mixture was subjected to mild vacuum degassing before casting. The resulting mixture was then poured into a mold coated with a releasing agent and allowed to cure at room temperature for 24 h, followed by post-curing in a hot air oven at 60 °C for four hours. The fibers were manually distributed during layup to achieve a random orientation, which was later confirmed through visual inspection of the fractured cross-section under SEM. Table 1 presents the composite designations with varying reinforcement concentrations, and Fig. 6 depicts the process flowchart of composite development.

Characterizations

The prepared specimen were cut into specified dimension for each test using water abrasive jet cutting machine in accordance with ASTM standards. Tensile, flexural, impact, hardness, ILSS, Interfacial shear strength (IFSS), thermal conductivity is the test performed to determine the strength and performance of the composite. Average of five specimens was tested for each test to ensure credibility and reliability. Table 2 shows the test done in this research and their specification. Figure 7 depicts the specimen prepared in this research.

Table 2 Test and their standards and machine specification

Test	ASTM standard	Specification
Tensile Flexural	D3039 (Dim: 250 × 25 mm) D790 (Dim: 120 × 12.5 mm)	Using a universal testing machine (UTM), the tensile and flexural properties were assessed. The durability of the composite was assessed by tensile testing, which involved securing dumbbell-shaped specimens in the machine and applying a load that pulled the specimen until it failed. A central force was applied, the specimen was put on the instrument, and the composite's resistance to bending was assessed for flexural strength.
Impact	D256 (Dim: 63.5 × 12.7 mm)	An impact tester made by Charpy was used to assess the impact resistance. V-notched specimens were positioned horizontally on the impact tester's support fixture and hit by a pendulum hammer. The composite's impact strength was calculated by measuring the energy absorbed during fracture.
Hardness	D2240 (Dim: 35 × 35 mm)	A hardness test was performed using the Shore-D durometer. The durometer indenter was uniformly pushed on the material while the specimens were on a level surface. The composite's resistance to localized deformation was revealed by this test.
ILSS	D2344 (Dim: 20 × 10 mm)	An ILSS test was performed using universal test machine. A rectangular specimen is loaded until shear failure between the laminate layers occurs in a short beam three-point bending configuration. This test assesses the interfacial bonding quality between the fiber and the matrix.
IFSS	No ASTM (Dim: 10 × 10 mm, embedded fiber length of 3 mm)	The single-fiber pull-out test was performed to evaluate the interfacial bonding between the fiber and polymer matrix. A single fiber was partially embedded in the polymer and cured, leaving one end free. The specimen was mounted in a micro-tensile testing setup, and a controlled tensile load was applied to pull the fiber out of the matrix. The maximum load recorded during debonding was used to assess the interfacial shear strength, providing a direct measure of fiber–matrix adhesion in the composite.
Thermal conductivity	D3850 (Dia 50 mm)	A steady heat flow was established by placing the disk-shaped specimen between heated and cooled plates. Using the measured temperature gradient, the thermal conductivity was determined in accordance with Fourier's law.
Water absorption	D570 (Dim: 60 × 60 mm)	Prior to testing, the prepared test specimens were weighed and then immersed in distilled water for two days. To determine the composite's water absorption percentage, the specimens were removed from the water, gently dried with a lint-free towel, and reweighed using a four-digit laboratory scale in accordance with ASTM standards.

Result and discussions

Mechanical properties of the composite

The stress-strain and load deflection curves are presented in Fig. 8 whereas, mechanical strength of the composites are analysed by conducting a test such as tensile, flexural, impact, ILSS, and hardness and it is represented in Fig. 9. The tensile, flexural and Inter laminar shear stress (ILSS) of the composite P, PNB0, PNB1, PNB2, and PNB3 was illustrated in graphical form in Fig. 9a, b, and d respectively. The composite P has 100 vol% of pure polyester composite without any reinforcement, which

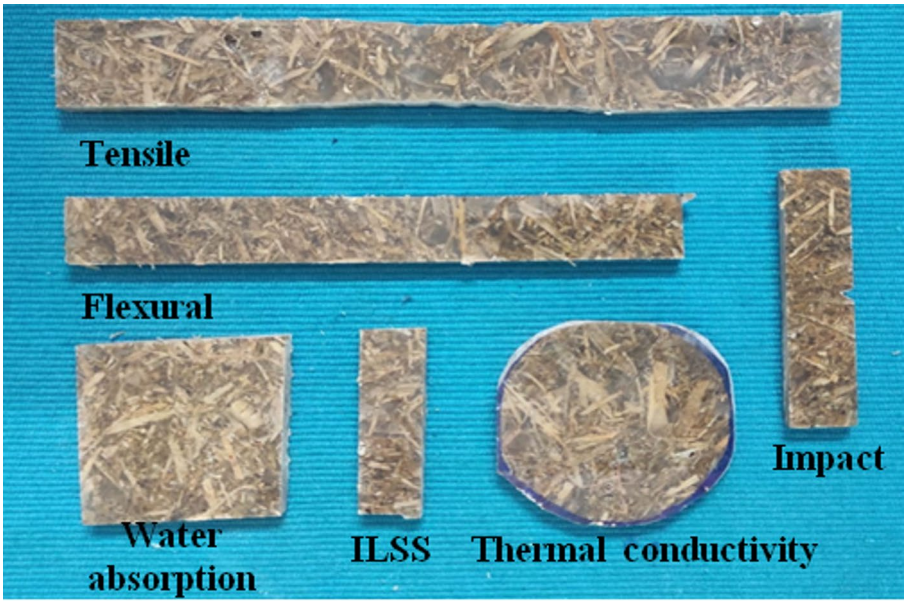

Fig. 7 Specimen prepared with ASTM standard

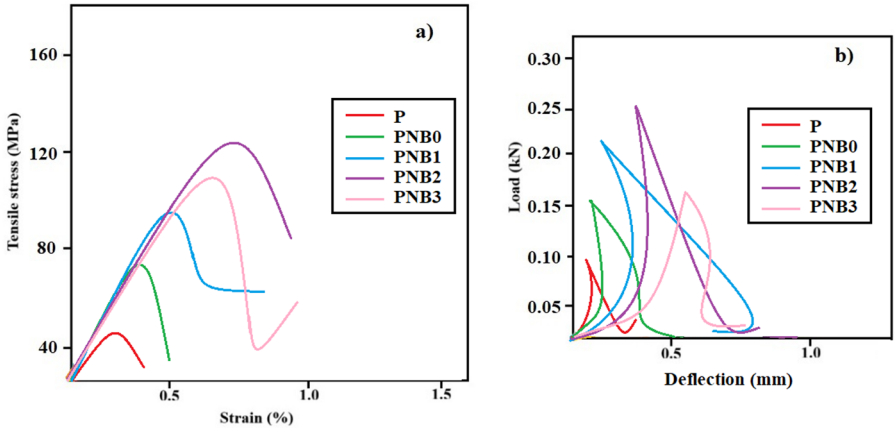

Fig. 8 (**a**) Stress-strain curve for tensile and (**b**) Load displacement curve for flexural test

exhibited good tensile strength of 46 MPa, flexural strength of 68 MPa and ILSS of 18 MPa respectively. Naturally, the polyester matrixes composite are having better flexibility, curing nature and good strength properties, however due to lack of reinforcement, forms gaps in the composite which reduce the material strength and further it is lower than other composites. The composite PNB0 with reinforcement of *Plumbago Zeylanica* stem fiber shows improved tensile, flexural, and ILSS strength of 73 MPa, 112 MPa, and 36 MPa respectively. The stem fiber of 40 vol% reinforcement provide better adhesion and silane treatment promotes strong interfacial

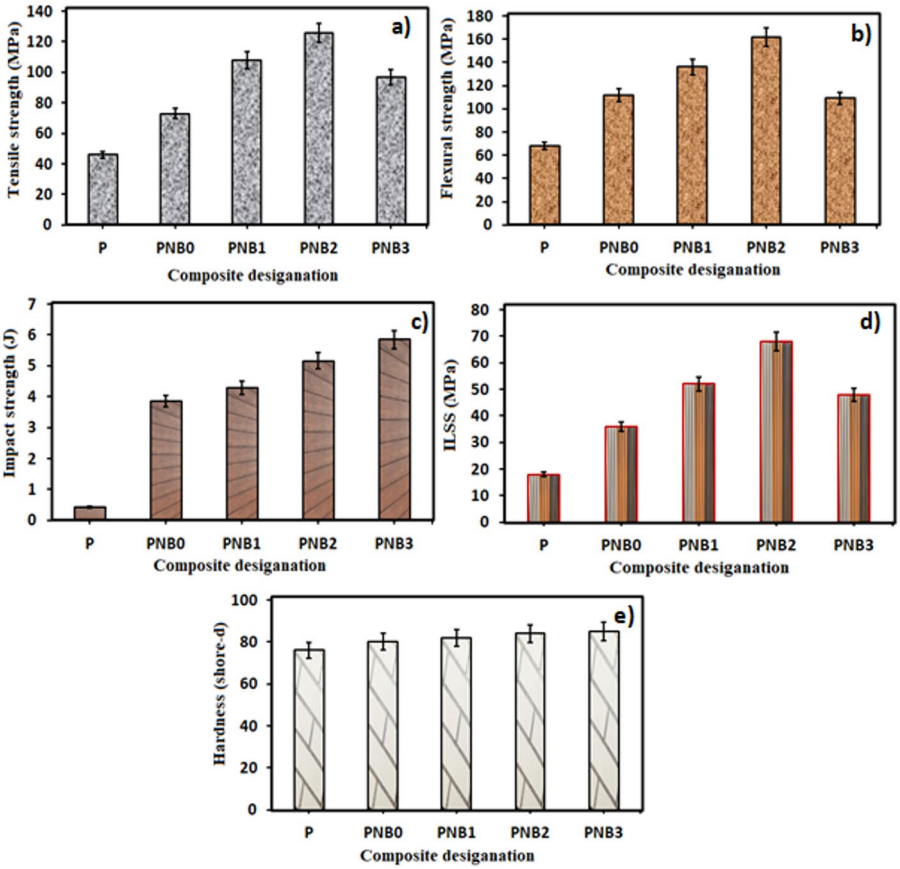

Fig. 9 Mechanical features of the prepared composite (**a**) Tensile strength (MPa), (**b**) Flexural strength (MPa), (**c**) Impact strength, (**d**) ILSS and (**e**) Hardness strength (shore-d)

bonding due to the presence of bonding agents such as hydroxyl and amine groups, this will enhance strength features of the composite [17]. Thus, when compared to plain polyester composite P, the fiber reinforced composite PNB0 show 58.69%, 64.70%, 100% better tensile, flexural, and ILSS strength respectively. Furthermore, the reinforcement of 1, 3, and 5 vol% of wheat straw extracted biosilica particle reinforced composite PNB1, PNB2, PNB3 shows enhanced tensile strength of 108 MPa, 126 MPa, and 97 MPa, flexural strength of 136, 162, and 109 MPa, and ILSS of 52 MPa, 66 MPa, and 48 MPa respectively. Biosilica after silane modification uniformly fills interfacial voids between fiber and matrix, reducing porosity, improves better load distribution, by acting as bridging of micro cracks formed during fiber filler reinforcement on matrix [18]. However, the PNB3 shows slight decline in tensile, flexural and ILSS strength because at 5 vol% biosilica particle forms agglomeration during reinforcement on matrix, this leads to uneven load bearing on the composite. Perhaps, it has also been evident that when compared to the plain poly-

ester composite P, the composite PNB3 shows 110.86%, 60.29%, 166.67% higher tensile, flexural and ILSS strength.

Similarly, the impact and hardness strength of the prepared composite are studied and it is represented in Fig. 9c) and e) respectively. The plain composite P shows low impact and hardness strength of 0.42 J, and 76 shore-d respectively. This is because the absence of fiber and filler, when subject sudden loading, the material experience low impact energy and surface rigidity of the composite experience low indented pressure withstanding capacity. Moreover, upon surface modified stem fiber (40 vol%) and biosilica (1, 3, 5 vol%) reinforcement on composite PNB0 and PNB1, PNB2, PNB3 shows maximum impact and hardness strength of 3.85 J, 4.28 J, 5.16 J, 5.85 J and 80, 82, 84, 85 shore-d respectively. The fiber filler under surface reinforcement provide better dispersion and better bonding strength which prevents the composite from debonding and improves impact and hardness properties of the composite [19]. Thus, when compared to plain composite specimen P, the composite PNB0, PNB1, PNB2, PNB3 shows improved impact energy and improved hardness strength.

The interfacial shear strength (IFSS) values of the composites clearly reflect the influence of fibre reinforcement, biosilica content, and surface modification on fibre–matrix interfacial integrity as shown in Fig. 10. The plain polyester composite (P) exhibits a negligible IFSS value, as it contains no reinforcing phase and therefore lacks a distinct fibre–matrix interface capable of transferring shear stresses. The composite PNB0, reinforced with 40 vol% silane-treated *Plumbago zeylanica* stem fibre, shows a substantial increase in IFSS to 12.8 MPa. This improvement is attributed to the silane treatment, which promotes chemical coupling between hydroxyl groups on the fibre surface and the polyester matrix, leading to enhanced interfacial adhesion and more efficient stress transfer across the interface. Further enhancement

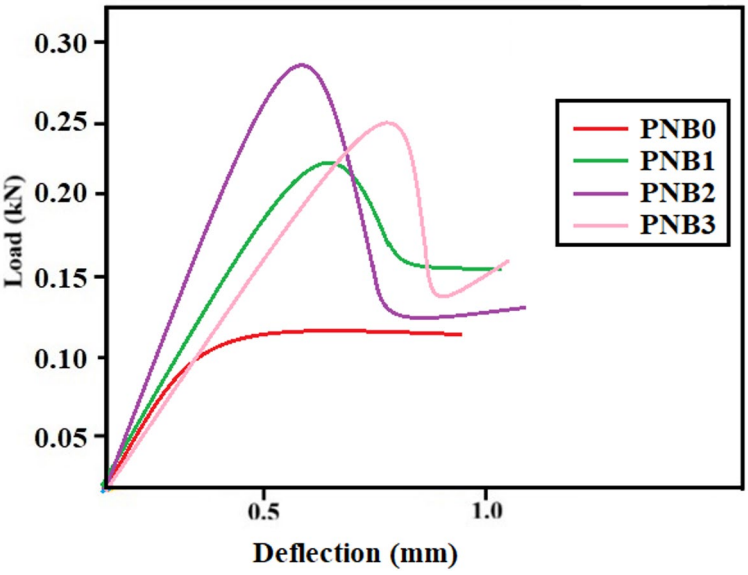

Fig. 10 Load displacement curve for IFSS

in IFSS is observed with the incorporation of silane-modified wheat straw derived biosilica particles. The PNB1 and PNB2 composites, containing 1 and 3 vol% biosilica, exhibit increased IFSS values of 14.6 MPa and 18.9 MPa, respectively. The finely dispersed biosilica particles effectively fill interfacial voids and micro-defects at the fibre–matrix boundary, reducing stress concentration and increasing mechanical interlocking. Additionally, the high surface area of biosilica facilitates improved load transfer by strengthening the interphase region and increasing the tortuosity of the shear path. However, a slight reduction in IFSS is observed for the PNB3 composite (16.4 MPa) containing 5 vol% biosilica. At higher filler loadings, biosilica particles tend to agglomerate, leading to non-uniform dispersion and the formation of weak interfacial regions. These agglomerates act as stress concentrators, hindering effective shear stress transfer and partially offsetting the benefits of increased filler content. Overall, the results indicate that an optimal biosilica loading (3 vol%) maximizes interfacial shear strength by balancing improved interfacial bonding and uniform dispersion, while excessive filler addition adversely affects interfacial performance due to agglomeration effects.

Table 3 presents the ANOVA for mechanical results to ascertain whether the reported results are statistically significant or not? With a p-value less than α, the null hypothesis (H0) is rejected. In some cases, the averages of the groups are not considered to be equal. Another way of putting it is that the disparity in the sample averages of certain groups is substantial enough to be considered statistically significant. The p-value is equal to 0.00000149287, and the probability that x is less than or equal to F is equal to 0.999999. In other words, the probability of making a type 1 error, which is the rejection of a true H0, is extremely low: 0.000001493 (0.00015%). The lower the p-value, the more strongly it supports the hypothesis H1. The value of the test statistic F is 18.79584, which is not inside the 95% acceptability range, which is represented by the equation [0: 2.8661]. f, the effect size that was detected, is quite large (1.94). This demonstrates that there is a significant disparity between the averages, which is a significant magnitude. The value of the η2 is equal to 0.79. According to this, the group is responsible for explaining 79% of the variance from the average, which is comparable to the R2 value in linear regression.

It is further noted that, according to the validation study, it is found that the H0 hypothesis is rejected, despite the fact that the priori power is low (0.1212). In order to determine whether or not the variances were equal, the program utilised Levene's test. It is believed that the variances of the population are comparable. There is a 0.0531 p-value. The test power of Levene is considered to be a low value (0.12). Consider the size of the groups to be comparable. "The ratio between the larger group and the smaller group is one," the statement reads. When the sizes of the groups are comparable, the analysis of variance (ANOVA) test is considered to be resilient to the assumption of homogeneity of variances. It is recommended that the Kruskal-

Table 3 ANOVA for mechanical results

Source	DF	Sum of Square	Mean Square	F Statistic	*P*-value
Groups (between groups)	4	37803.0496	9450.7624	18.7958	**0.000001493**
Error (within groups)	20	10056.2279	502.8114		
Total	24	47859.2775	1994.1366		

Wallis analysis of variance (ANOVA) non-parametric test be considered. Using the Shapiro-Wilk Test, the assumption was examined to ensure its validity. ($\alpha = 0.05$). For a minor breach of the normality assumption, the analysis of variance (ANOVA) test is regarded to be robust. The p-value for one of the groups that has a tiny sample size, which is less than 30, is 0.0104, which indicates that the group does not distribute normally.

Utilising the Kruskal–Wallis non-parametric test or transforming the data is something you ought to think about doing.

In continuation with statistical validation, the scanning electron microscope results significance insights. Figure 11(a-d) represents scanning electron microscopy (SEM) features of the composites to provide better view of the fiber matrix bonding adhesion. Figure 11a) depicts the plain polyester composite P, when subjected load, the material get distort quickly because of lack of reinforcement. Figure 11b) demonstrates composite PNB0, better fiber and matrix reinforcement, improved the load carrying capacity because of surface modification process done over the natural stem fiber. Further, surface modified biosilica particle reinforcement along with the fiber provide better dispersion and even load distribution throughout the composite PNB1 shows in Fig. 11c), which leads to improved tensile strength. Figure 11d) represents the composite PNB2 with reinforcement of 3 vol% of biosilica particle, increase in optimal filler concentration and surface modification provide strong bonding arrangements of fiber filler and polymer matrix, this in turn promote overall mechanical qualities of the composite [20, 21]. Figure 11e) represents the composite PNB3, which shows an agglomeration of filler particle, improper binding of fiber and filler into matrix, leads to uneven load distribution, leads to slight decline in mechanical strength features of the composite.

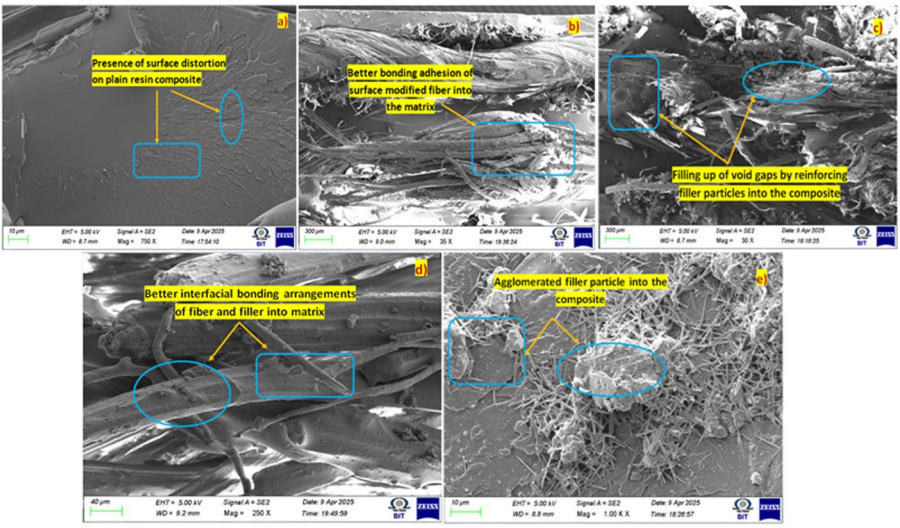

Fig. 11 scanning electron microscopy analyses of composites (**a**) P, (**b**) PNB0, (**c**) PNB1, (**d**) PNB2, (**e**) PNB3

Thermal conductivity properties of the composite

Thermal conductivity behaviour of surface modified *Plumbago zeylanica* stem fiber and biosilica particle reinforced composite are evaluated and it is represented in Fig. 12. The plain polyester composite P, the polymer network channels, with no fiber and filler shows low heat conductivity region throughout the composite of 0.278 W/m-K. The reinforcement silane treated fiber substance into the composite PNB0 shows improved thermal conductivity of 0.572 W/m-K and it is 105.7% better conductivity compared to base specimen P, it is primarily due to the optimized interface, better dispersion, and effective heat transfer network established by the silane-treated fiber. The intrinsic heat conductivity of reinforcing fibers can be significantly higher than that of the underlying polymer [22]. They can create a more effective thermal channel when they are evenly distributed and bound. The fibers are more successfully aligned or integrated into the composite structure attributed by the silane treatment.

Furthermore, the reinforcement of 1, 3, 5 vol% of biosilica particle along with the fiber enhanced the thermal conductivity of the composite PNB1, PNB2, PNB3 of values 0.682, 0.772, 0.861 W/m-K respectively. Biosilica particles, due to their ceramic-like nature, possess relatively high intrinsic thermal conductivity. When well-dispersed in the matrix, they act as effective heat conductors. Thus, the presence of both silane-treated fibers and well-distributed biosilica particles improves the interfacial bonding with the matrix. This reduces interfacial thermal resistance, enhancing the flow of heat through the composite [23]. This shows that when compared to the plain polyester composite, the fiber filler reinforced composite PNB1, PNB2, PNB3 exhibited 19.2%, 35%, 50.5% better thermal conductivity.

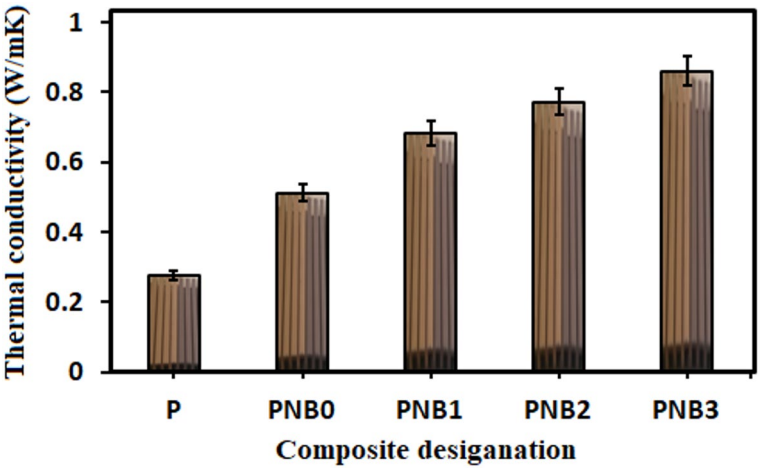

Fig. 12 Thermal conductivity behaviour of the composite

Water absorption

The water absorption behaviour of the composites as a function of immersion time is presented in Fig. 13. All specimens exhibited a progressive increase in water uptake with increasing immersion duration, indicating a diffusion-controlled absorption mechanism. The plain polyester composite (P) showed the highest water absorption at all time intervals, reaching 0.18%, 0.25%, 0.30%, and 0.34% after 12, 24, 36, and 48 h, respectively. This comparatively higher moisture uptake is attributed to the inherent permeability of the neat polyester matrix and the absence of reinforcements or fillers capable of obstructing water diffusion pathways. In comparison, composites reinforced with 40 vol% surface-modified stem fiber (PNB0) and those additionally incorporating surface-modified biosilica particles (PNB1–PNB3) exhibited consistently lower water absorption throughout the exposure period. At 48 h, the water absorption decreased from 0.32% for PNB0 to 0.28%, 0.25%, and 0.21% for PNB1, PNB2, and PNB3, respectively. A similar decreasing trend was observed at intermediate immersion times (12–36 h), confirming the sustained effectiveness of surface treatment and filler incorporation in restricting moisture ingress.

The observed reduction in water uptake is primarily attributed to the silane treatment, which improves chemical bonding between the fiber/particle surfaces and the polyester matrix, thereby reducing interfacial voids and micro-gaps that typically act as preferential sites for water penetration [24]. Additionally, the incorporation of biosilica particles contributes to void filling within the matrix and at the fiber–matrix interface, resulting in a denser and more compact microstructure with reduced porosity. The increased biosilica content enhances the tortuosity of diffusion pathways, effectively limiting water transport through the composite thickness [25]. Among all compositions, the PNB3 composite exhibited the highest resistance to moisture absorption, demonstrating approximately 38.23% lower water uptake compared to the plain polyester composite after 48 h of immersion. This improved hydrophobic behaviour highlights the synergistic effect of surface-modified stem fibers and biosil-

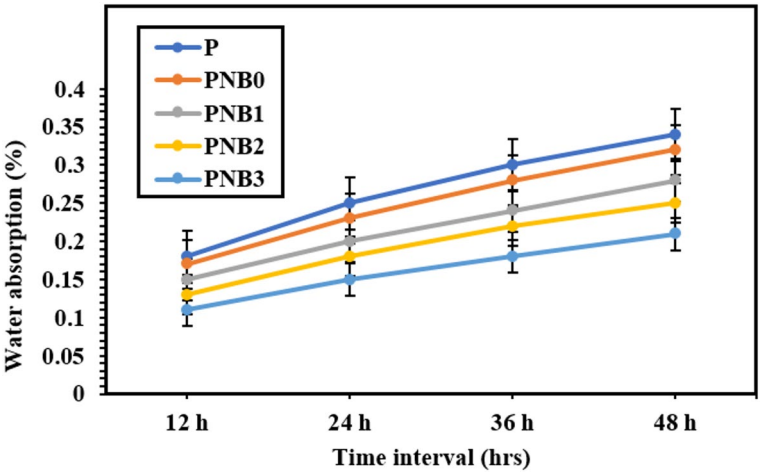

Fig. 13 Water absorption characteristics of the composite

Table 4 Comparison with prior research works

Author	Research	Results
Arun Prakash et al. [26]	Mechanical, Thermal, and Fatigue Behavior of Epoxy Composites Reinforced with Surface-Treated *Caryota urens* Fibre.	The epoxy composite reinforced with silane-treated *Caryota urens* fibre demonstrates the highest interlaminar shear strength of 28 MPa and exhibits enhanced fatigue resistance, attaining a maximum fatigue life of 18,315 cycles at 25% of the ultimate tensile stress.
Mathu et al. [27]	Mechanical, Thermal Conductivity, and Dielectric Behavior of Polyester Composites Reinforced with Silane-Modified Sugarcane Bagasse Biochar and Flax Fibre.	Among the composites studied, specimen EFB2 (3 vol% biochar with 40 vol% fibre) exhibits the most balanced mechanical performance, attaining a tensile strength of 138 MPa, a flexural strength of 151 MPa, and an impact energy of 6.7 J.
Alshaharani et al. [28]	Influence of Silane-Grafted Orange Peel Biochar and Areca Fibre on the Mechanical, Thermal Conductivity, and Dielectric Characteristics of Epoxy Composites.	The composite shows substantial mechanical improvement, with tensile and flexural strengths enhanced by 64% and 50%, respectively, while impact resistance increases by approximately 93%. Furthermore, the RAB3 formulation attains the highest thermal conductivity, measuring 0.426 W/mK.

ica fillers, making the developed composites more suitable for applications requiring enhanced durability and dimensional stability under humid or moisture-rich service environments.

Comparative analysis

This subsection concludes the comparative analysis with the similar prior research works which are presented in Table 4.

Conclusions of the research study

The research concludes that reinforcement of silane treated *Plumbago zeylanica* stem fiber and biosilica particle reinforced composite shows better mechanical, thermal conductivity, and water absorption properties.

- The silane modified stem fiber of 40 vol% and 3 vol% of silane treated biosilica particle into the composite PNB2 shows maximum tensile, flexural, ILSS, IFSS strength of 126 MPa, 162 MPa, 68 MPa, 18.9 MPa and it is 173.9%, 138.2%, 277.8% better than plain composite P. This improved strength features is mainly because of better bonding strength of silane treated fiber/ filler into the matrix.

However, the composite PNB3 with reinforcement of 5 vol% of modified biosilica shows maximum impact and hardness strength of 5.85 J, and 85 shore-d.

- Similarly, the same composite PNB3 with that volume percent of surface treated fiber and filler shows maximum thermal conductivity of 0.861 W/m-K and reduced water absorption rate of 0.21% and it is 209.7%, 61.9%, better than plain composite P.
- This conductivity and reduced moisture absorption is because of presence of both silane-treated fibers and well-distributed biosilica particles improves the interfacial bonding with the matrix. This reduces interfacial thermal resistance, enhancing the flow of heat through the composite and lowers porosity, limiting the pathways for water diffusion.
- Thus, the present research study is significance by infusing silane treatment on fiber and filler particle, which provide better bonding adhesion composite, promote better load distribution and this fiber and fillers are extracted from natural waste which converts waste biomass into useful product.
- This light weight, better mechanical and thermal conductivity, better water absorption properties of composites could potentially be applied in areas such as automotive, aviation, various industrial, domestic household, civil engineering application, etc.

Acknowledgements Nil.

Author contributions P Subash, P Gurusamy – Research. V. Muthuraman - writing and testing. S. Vijayan – Material arrangement and writing.

Funding Nil.

Data availability No datasets were generated or analysed during the current study.

Declarations

Competing interests The authors declare no competing interests.

Ethical approval NA.

References

1. Kumar S, Saha A (2022) Proceedings of the Institution of Mechanical Engineers, Part C: Journal of Mechanical Engineering Science. 236(3):1733-50 https://doi.org/10.1177/09544062211023105
2. Balogun OP, Sanusi KO, Jeje SO, Faola AE, Majolagbe SB, Iyamu-Okoeguale SO (2023) J Polym Res 30(6):235. https://doi.org/10.1007/s10965-023-03614-9
3. Okafor CE, Kebodi LC, Kandasamy J, May M, Ekengwu IE (2022) Compos Part C: Open Access 7:100213. https://doi.org/10.1016/j.jcomc.2021.100213
4. Joe MS, Sudherson DPS, Suyambulingam I, Siengchin S, Rajeshkumar G (2023) Biomass Convers Biorefinery 13(15):14267–14280. https://doi.org/10.1007/s13399-023-04379-3
5. Saha A, Kumari P (2022) Mater Today Commun 31:103800. https://doi.org/10.1016/j.mtcomm.2022.103800

6. Ponnusamy M, Natrayan L, Kaliappan S, Velmurugan G, Thanappan S (2022) Adsorption Science & Technology, 2022, 4268314. https://doi.org/10.1155/2022/4268314
7. Venkatesh R, Logesh K, Singh PK, Mohanavel V, Singh S, Soudagar MEM, Obaid SA (2025) Journal of Mechanical Science and Technology, pp: 1–7. https://doi.org/10.1007/s12206-024-1216-4
8. Lakshmipathi AR, Satishkumar P, Nagabhooshanam N, Rao PKV, Kumar DS, Chakravarthy AK, Mohanavel V (2025) Biomass Conversion and Biorefinery, 15(2):2893–2901. https://doi.org/10.1007/s13399-023-04854-x
9. Saha A, Kumari P (2023) Polym Compos 44(4):2449–2473. https://doi.org/10.1002/pc.27256
10. Diharjo K, Andoko A, Soedarsono JW, Gapsari F, Rangappa SM, Siengchin S (2025) Results Eng 104260. https://doi.org/10.1016/j.rineng.2025.104260
11. Jenish I, Felix Sahayaraj A, Appadurai M, Fantin Irudaya Raj E, Suresh P, Raja T, Manikandan V (2021) Advances in Materials Science and Engineering, 2021(1), 6078155. https://doi.org/10.1155/2021/6078155
12. Balaji KV, Shirvanimoghaddam K, Yadav R, Ferdowsi MRG, Naebe M (2024) Hybrid Adv 6:100253. https://doi.org/10.1016/j.hybadv.2024.100253
13. Ponphaiboon J, Krongrawa W, Aung WW, Chinatangkul N, Limmatvapirat S, Limmatvapirat C (2023) Molecules 28(13):5163. https://doi.org/10.3390/molecules28135163
14. Huang L, Yu F, Liu Y, Lu A, Song Z, Liu W, Zhu C (2023) Composites Science and Technology, 233,109905. https://doi.org/10.1016/j.compscitech.2022.109905
15. Raghunathan V, Gnanasekaran S, Ayyappan V, Devanathan LS, Rangappa M, S., Sienghcin S (2024) Polym Compos 45(11):10204–10219. https://doi.org/10.1002/pc.28467
16. Li X, Sun J, Shao S, Yan J, Cai Y (2023) Renewable Energy 206:506–513. https://doi.org/10.1016/j.renene.2023.02.031
17. Saha A, Kulkarni ND, Kumari P (2024) Constr Build Mater 441:137486. https://doi.org/10.1016/j.conbuildmat.2024.137486
18. Mohammadi M, Ishak MR, Sultan MTH (2024) J Nat Fibers 21(1):2408633. https://doi.org/10.1080/15440478.2024.2408633
19. Gayathri N, Pragadish N, Jothi GA,S, S. K (2024) Silicon 16(11):4647–4657. https://doi.org/10.1007/s12633-024-03024-6
20. Saha A, Kulkarni ND, Kumari P, Environment (2025) Dev Sustain 27(5):10655–10691. https://doi.org/10.1007/s10668-023-04327-1
21. Dhilip JDJ, Raghunathan V, Mohan R, Ayyappan V, Rangappa SM, Siengchin S (2024) Biomass Conversion and Biorefinery, pp: 1–14. https://doi.org/10.1007/s13399-024-06124-w
22. Saha A, Kulkarni ND, Kumar M, Kumari P, Biomass (2024) Convers Biorefinery 14(20):26247–26266. https://doi.org/10.1007/s13399-023-04709-5
23. Kandavalli SR, Sahu SK, Chanakyan C (2024) J Vinyl Additive Technol 30(4). https://doi.org/10.1002/vnl.22095
24. Bagla A, Kulkarni ND, Kumari P, Saha A (2025) ACS Appl Polym Mater 7(9):5584–5597. https://doi.org/10.1021/acsapm.5c00408
25. Vijayaraj S, Vijayarajan K (2024) Biomass Convers Biorefinery 14(17):21485–21495. https://doi.org/10.1007/s13399-023-04638-3
26. Arun Prakash VR, Xavier JF, Ramesh G, Maridurai T, Kumar KS, Raj RB (2022) Biomass Convers Biorefinery 12(12):5451–5461. https://doi.org/10.1007/s13399-020-00938-0
27. Mathu DS, Sudherson DP (2025) Transactions on Electrical and Electronic Materials. Jul 9:1–1. https://doi.org/10.1007/s42341-025-00642-8
28. Alshahrani H, Prakash VA, Biomass Conversion (2024) and Biorefinery. 14(6):8081–8089. https://doi.org/10.1007/s13399-022-02801-w

Authors and Affiliations

P. Subash[1] · P. Gurusamy[1] · V. Muthuraman[2] · S. Vijayan[3]

✉ P. Gurusamy
gurusamyp@citchennai.net

[1] Department of Mechanical Engineering, Chennai Institute of Technology, Chennai, India

[2] Department of Mechanical Engineering, Vels Institute of Science, Technology and Advanced Studies (VISTAS), Chennai, India

[3] Department of Mechanical Engineering, Sri Sivasubramaniya Nadar College of Engineering, Chennai, India